BMC Cancer

RESEARCH

Open Access

Ex vivo engineering of phagocytic signals in breast cancer cells for a whole tumor cell-based vaccine

Román Martí-Díaz[1], Luis Sánchez-del-Campo[1], María F. Montenegro[1], Trinidad Hernández-Caselles[2], Antonio Piñero-Madrona[3], Juan Cabezas-Herrera[4*] and José Neptuno Rodríguez-López[1*]

Abstract

Background Today, cell therapies are constantly evolving and providing new options for cancer patients. These therapies are mostly based on the inoculation of immune cells extracted from a person's own tumor; however, some studies using whole tumor cell-based vaccines are approaching the level of maturity required for clinical use. Although these latest therapies will have to be developed further and adapted to overcome many ethical barriers, there is no doubt that therapeutic cancer vaccines are the next frontier of immunotherapy.

Methods Ionizing radiation and CD47 knockout via CRISPR-Cas9 genome editing were used to optimize the macrophage-mediated phagocytosis of breast cancer cells. These cells were subsequently used in several mouse models to determine their potential as novel whole-cell-based vaccines to drive antitumor immunity. To improve the recognition of tumor cells by activated immune cells, this cellular therapy was combined with anti-PD-1 antibody treatments.

Results Here, we showed that irradiation of 4T1 breast cancer cells increases their immunogenicity and, when injected into the blood of immunocompetent mice, elicits a complete antitumor immune response mediated, in part, by the adaptive immune system. Next, to improve the macrophage-mediated phagocytosis of breast cancer cells, we knocked out CD47 in 4T1 cells. When injected in the bloodstream, irradiated CD47 knockout cells activated both the adaptive and the innate immune systems. Therefore, we used these ex vivo engineered cells as a whole tumor cell-based vaccine to treat breast tumors in immunocompetent mice. A better response was obtained when these cells were combined with an anti-PD-1 antibody.

Conclusion These results suggest that tumor cells obtained from surgical samples of a breast cancer patient could be engineered ex vivo and used as a novel cell therapy to drive antitumor immunity.

Keywords Breast cancer, Whole tumor cell-based vaccines, CD47, Ionizing radiation, Anti-tumor immunity

*Correspondence:
Juan Cabezas-Herrera
juan.cabezas@carm.es
José Neptuno Rodríguez-López
neptuno@um.es
[1]Department of Biochemistry and Molecular Biology A, School of Biology, University of Murcia, IMIB-Pascual Parilla, Murcia 30100, Spain
[2]Department of Biochemistry and Molecular Biology B and Immunology, Faculty of Medicine, University of Murcia, IMIB-Pascual Parilla, Murcia, Spain
[3]Department of Surgery, University Hospital Virgen de la Arrixaca, University of Murcia, IMIB-Pascual Parilla, Murcia, Spain
[4]Translational Cancer Research Group, University Hospital Virgen de la Arrixaca, IMIB-Pascual Parilla, Murcia, Spain

Introduction

Cancer cell therapy has become one of the most promising approaches for the treatment of cancer [1]. In recent years, progress in the underlying science, clinical application and manufacturing of cell therapies has accelerated dramatically. CAR T-cell therapy has shown some success in treating hematological tumors, but several challenges, such as antigen selection, tolerability and safety, remain in the treatment of solid tumors [2]. Multiple approaches are now exploring different immune cell types as therapeutic platforms, and genetic clinical approximations are related to treatment with immune cells [3, 4]; less common is the use of whole cancer cells as therapeutic vaccines [5–7]. Recently, AGI-101 H, an allogeneic gene-modified whole-cell therapeutic melanoma vaccine, has been evaluated in more than 400 melanoma patients in the adjuvant and therapeutic settings (EudraCT Number 2008–003373-40) [8]. In this context, we observed that ex vivo irradiation of melanoma cells efficiently induced immune suppression of melanoma tumor formation, and this antimelanoma immune response was mediated by the adaptive immune system [9]. Interestingly, a vaccination assay in which immunocompetent animals were immunized by tail vein injection of irradiated B16/F10 cells demonstrated a substantial protective immune response against subcutaneously inoculated B16/F10 cells [9].

Although the interaction of the immune system with a malignant tumor is extremely complex, many studies have elucidated how some tumors can escape surveillance and destruction by the immune system. With respect to the activation of the acquired immune system, insufficient and/or defective presentation of tumor-associated antigens by antigen-presenting cells (APCs) constitutes an important mechanism of immune tolerance [10]. APCs, which include dendritic cells (DCs), monocytes/macrophages and activated B cells, play a major role in full T-cell activation. DCs must have the capacity to process and present tumor-associated antigens to both $CD4^+$ and $CD8^+$ T cells. In this scenario, because the activation of APCs requires direct cell–cell contact with tumor cells, the regional location of epithelial tumors and the poor accessibility of these APCs to the tumor environment could represent a first barrier to appropriate antigenic presentation. In addition, other mechanisms that result in an unfavorable ratio of "eat me" versus "do not eat me" signals on the surface of tumor cells [such as calreticulin (CALR) and CD47, respectively] also impede their phagocytosis by APCs [11, 12], which is necessary for tumor antigen presentation. Although therapies to increase the recognition and phagocytosis of tumor cells by APCs have been widely exploited with the use of radiotherapy [13] and/or antibodies against CD47 [14], increasing the accessibility of APCs to the cell environment, conceptually, is a more difficult task. On the other hand, independent of the level of $CD8^+$ T-cell activation, tumor cells frequently escape $CD8^+$ T-cell recognition and $CD8^+$ T-cell-induced death by activating "don't find me" signals [15–17]. Among other mechanisms, programmed cell death-ligand 1 (PD-L1), which is expressed by tumor cells, plays a critical role in the induction of inhibitory signals through interactions with programmed cell death-1 (PD-1), which is expressed on the cell surface of T cells [18, 19]. This PD-1/PD-L1 interaction results in the suppression of tumor-specific T-cell responses, functioning as a tumor immune evasion mechanism. Therefore, ideally, immunotherapy strategies should focus on increasing the processing and presentation of antigens while enhancing T-cell killing of tumor cells, for example, by using immune checkpoint blockade with anti-PD-L1/PD-1 antibodies [20].

In the present study, we evaluated a new concept for immunotherapy that could be summarized as follows: "If the APCs do not come to tumor cells, tumor cells will travel to the APCs" to design an experimental therapy for breast cancer in animal models. In the first step, we manipulated breast cancer cells ex vivo to produce more immunogenic cells; we worked on a proof-of-principle that the injection of ex vivo manipulated tumor cells could be an efficient therapy for breast cancer. Then, we combined this cellular therapy with anti-PD-1 treatments to improve the recognition of tumors by activated immune cells. Since clinical trials are currently being conducted with whole tumor cell-based vaccines [7, 8], the clinical translation of the therapeutic approach proposed here could lead to personalized immunotherapies to improve the clinical outcomes of patients with breast cancer.

Methods

Antibodies

The following antibodies were used: β-actin (Merck, Madrid, Spain; monoclonal clone AC-15; A5441), CALR (Thermo-Fisher, Barcelona, Spain; mouse monoclonal; MA5-11723), CD3-APC (Cytek Biosciences, Fremont, CA, USA; clone 17A2, 17-0032-80), CD3-FITC (Biolegend, San Diego, CA, USA; clone 145-2C11, 100305), CD8 (Thermo-Fisher, 14-0081-82), CD8-PE (Thermo-Fisher, 12-0081-82), CD47 (Novus Biologicals, Englewood, CO, USA), FOXP3 (Thermo-Fisher, 14-5773-82), NKp46 (Thermo-Fisher, PA5–79720), NKp46-APC (Biolegend, clone 29A1.4, 137607), and PD-L1 (Thermo-Fisher, 14-59-82-82).

Cell culture and treatments

The 4T1 mouse breast cancer cell line was tested for mycoplasma and cultured according to the ATCC guidelines. 4T1-luc2 cells were obtained from Caliper Life

Sciences (Hopkinton, MA, USA) and cultured in 5% CO_2 at 37 °C with 1% penicillin–streptomycin DMEM plus 10% fetal bovine serum (FBS). Dr. Detlef Schuppan kindly provided YAC-1 cells [21]. Cell proliferation was evaluated using the MTT analysis. In these tests, the cells were placed in 96-well plates with a density of 1000–2000 cells/wells. For ionizing radiation (IR) assays, the cells were irradiated at a 10 Gy dose using an Andrex SMART 200E machine (YXLON International, Hamburg, Germany) operating at 200 kV, 4.5 mA with a focus–object distance of 20 cm at room temperature and a dose rate of 10 Gy. In a radiation cabin, the radiation doses were tracked using a UNIDOS universal dosimeter in a PTW Farme ionization chamber TW 30,010 (PTW-Freiburg, Freiburg, Germany).

Mice

Female BALB/c, Rag2/IL2RG (R2G2), and Athymic Nude-Foxn1nu mice (4–5 weeks of age) were obtained from Envigo (Barcelona, Spain). The mice were kept in a particular pathogen-free animal facility at the University of Murcia under aseptic conditions (positive air pressure in a mouse room with microisolator tops), and a laminar flow hood was used for all mouse handling operations [22]. We made every attempt to reach the conclusion using as small a sample size as possible. Prior to conducting experiments, we typically eliminate samples if we notice any abnormalities in the mice's size, weight, or apparent disease symptoms; however, we did not exclude any animals in this study because we did not find any abnormalities. Neither blinding nor randomization were used in this investigation.

Animal models

To establish primary breast tumors, 5×10^5 4T1-luc2 cells (irradiated or not irradiated) in 50 µl of PBS were injected into the mammary fat pads of BALB/c mice using a 27-gauge needle. For the metastasis colonization experiments, the indicated 4T1 cells (5×10^5) expressing or not expressing luciferase were injected intravenously into the mice through the tail vein or into the arterial blood supply (intracardiac inoculation) of the indicated mice. For the vaccination experiments, vehicle (PBS) or the indicated 4T1 cells (5×10^5) expressing luciferase were injected intravenously into BALB/c mice through the tail vein. After four weeks, 5×10^5 4T1-luc2 cells were injected into the mammary fat pad as indicated above. For the treatment of primary preformed breast tumors with whole cancer cells, primary tumors were established with non-irradiated 4T1-luc2 cells. After three weeks, vehicle (PBS) or the indicated 4T1 cells (5×10^5) expressing luciferase were injected intravenously into the mice through the tail vein. For PD-1 blockade experiments, 200 µg anti-PD-1 (donated by Prof. Yagita) was administrated intraperitoneally on days 21, 26, and 31 after breast tumors implantation (time zero). Tumors and organs colonization by luciferase-containing cells was analyzed in mice anesthetized with isoflurane (1.5-2% delivered in 100% O_2 at 1 l/min) using the IVIS Imaging System (Caliper Life Sciences, Hopkinton, MA, USA). Lung colonization of 4T1 cells not expressing luciferase was revealed by hematoxylin and eosin (H&E) stain. Mice were euthanized after indicated days by isoflurane overdose followed by cervical dislocation.

Mouse-derived breast tumors

Fresh tumor samples obtained from the indicated mice were used for protein and mRNA extraction. Sections of fresh samples were kept at -80 °C until they were needed. As explained below, three randomly selected slices from each tumor were utilized for protein extraction and three more slices were used for phenol–chloroform-mediated total RNA extraction. Western blot analysis was performed using a pool of protein extracts. Equal amounts of the three cDNA fractions corresponding to the same tumor were pooled and utilized for real-time RT-PCR quantification of PD-L1 mRNA after cDNA was synthesized using RNA (5 µg) (see below). Formalin-fixed, paraffin-embedded, mouse-derived tumors were employed for IHC analyses (see below).

CRISPR/Cas9 CD47 knockout

We used CRISPR/Cas9 protocols to generate 4T1-luc2-CD47-KO cells. In a 6-well plate, the cells were grown to 60–70% confluency and transfected with the Santa Cruz Biotechnology (Dallas, TX, USA) plasmid CD47 CRISPR/Cas9, which contained the indicated specific gRNA sequences, the Cas9 ribonuclease (CD47m SC-421654-KO), and its HDR plasmids (CD47m SC-400401-HDR). Transfection was performed via the FuGENE6 reagent (Promega, Madison, WI, USA), and a 1:3 DNA/FuGENE6 ratio. The transfection medium was maintained for 48 h. On day 2, the transfection medium was removed, and puromycin-containing fresh medium (5 µg/mL) was added to the cells. The cells were then allowed to grow for three more days. Single-cell colonies were isolated and grown after five to six days. Western blot tests and Sanger sequencing were performed after genomic DNA extraction to define positive clones. To check for potential off-target effects, we performed an analysis of the gRNA used in our CRISPR experiments using the web tool for genome editing CRISPOR.org that scores and evaluates the potential off-targets in the genome derived from the gRNA sequence. This analysis resulted in specificity scores of 98/100 for MIT and 98/100 for CFD. The higher the specificity score, the lower off-target effects in the genome. The specificity

score ranges from 0 to 100 and measures the uniqueness of a guide in the genome.

PCR analysis

Standard operating procedures were followed for mRNA extraction, cDNA synthesis, and both conventional and quantitative real-time RT-qPCR. Thermo Fisher Scientific generated the primers after designing them with Primer Express version 2.0 software. The following primers for mouse genes were used: β-actin (forward: 5′-AGA AAA TCT GGC ACC ACA CC-3′; reverse: 5′-GGG GTG TTG AAG GTC TCA AA-3′); PD-L1 (forward: 5′-GAC CAG CTT TTG AAG GGA AAT G-3′; reverse: 5′-CTG GTT GAT TTT GCG GTA TGG-3′). Reactions were performed in SYBR Green mix (Applied Biosystems, Foster City, CA, USA) using the QuantStudio 5 Real-Time PCR System (Applied Biosystems). The $2^{-\Delta\Delta Ct}$ method was used to evaluate the data, and the relative levels of mRNA expression were adjusted to those of β-actin [22].

Confocal microscopy and immunofluorescence procedures

Using a laser-scanning inverted confocal microscope (Leica TCS 4D, Wetzlar, Germany), fluorescence staining imaging was performed by confocal imaging of fixed cells. The samples were imaged using a 63×/1.4 numerical aperture oil objective. Cells were cultured on 100 mm^2 coverslips, fixed in 3% paraformaldehyde, and permeabilized with 0.2% Triton X-100 for indirect immunofluorescence analysis. Coverslips were incubated in 5% bovine serum albumin (BSA) for 20 min and probed with primary antibodies (diluted 1:200 in PBS containing 5% BSA) overnight at 4 °C. Next, the cells were washed three times in PBS and incubated for 2 h at room temperature with Alexa Fluor Dyes [Alexa Fluor 488-conjugated goat anti-mouse IgG (H + L) (A11001) and Alexa Fluor 633-conjugated goat anti-rabbit IgG (H + L) (A21071), both from Thermo Fisher]. Coverslips were permanently mounted to the slides using fluorescent mounting medium (PROLONG-GOLD, Thermo Fisher Scientific).

Histology and immunohistochemistry

After being extracted, the lungs were cleaned in PBS and preserved in 10% formalin. Serial slices of tissues fixed in paraffin were subjected to standard H&E staining. A Nikon Eclipse 90i light microscope was used to take pictures of the stained sections, and ImageJ software was used to analyze the pictures. For immunohistochemistry, paraffin sections were deparaffinized and subjected to antigen retrieval in sodium citrate buffer (pH 6.0). Hydrogen peroxide (5%) was used to deactivate the tissue's endogenous peroxidase. The slices were blocked and incubated overnight at 4 °C with the indicated primary antibodies. Next, the slices were incubated with secondary antibodies conjugated with peroxidase, and specific reactions were developed with 0.2% diaminobenzidine tetrahydrochloride and hydrogen peroxide.

Western blots

The SDS-PAGE sample loading buffer was added to collect whole-cell lysates. The proteins were separated by SDS-PAGE, transferred to nitrocellulose membranes, and examined by immunoblotting (WesternBright Quantum, Advansta, San Jose, CA, USA) after the samples had been sonicated and boiled for 10 min. Mouse-derived tumors were removed, washed twice in PBS, and immediately frozen at -80 °C. After thawing, the tumors were chopped into approximately 0.2 g pieces to increase the exposed surface area and then homogenized in buffer [10 mM PBS pH 7.4, 1% NP-40, 150 mM NaCl, 0.5% sodium deoxycholate, 0.1% SDS (w/v), and protease inhibitor cocktail] using polytron and Potter homogenizers. Proteins in these extracts were analyzed by Western blotting as described above. For quantification, the Western blot results were scanned with a Bio-Rad ChemiDoc scanning densitometer (Bio-Rad Laboratories, Hercules, CA).

Phagocytosis assay

Mouse peripheral blood mononuclear cells (PBMCs) were isolated from the whole blood of BALB/c mice using Histopaque-1077 (Merck) and resuspended in RPMI 1640 supplemented with 10% (v/v) FBS, 1% penicillin–streptomycin, and 2 mM L-glutamine in 10% CO_2 at 37 °C. Isolated PBMCs were seeded in 12-well plates for 2 h at 37 °C and 10% (v/v) CO_2 to allow the monocytes to adhere to the plate. Nonadherent cells were removed, and the monocytes were incubated with fresh complete media containing M-CSF (100 ng/ml; ThermoFisher) for an additional 21 days to allow full differentiation into macrophages. On the day of the phagocytosis assay, the 4T1 cells were fluorescently labeled with carboxyfluorescein succinimidyl ester (CFSE) (Thermo Fisher) in green, and the macrophages were labeled with PKH26 (Merck) in red according to the manufacturer's protocol. CFSE-labeled 2×10^5 4T1 cells were incubated with 10 μg/ml CD47 blocking antibody (Bio-XCell, West Lebanon, NH, USA, BE0283) or isotype control in 1 ml of serum-free DMEM at 37 °C and 7.5% (v/v) CO_2 with rotation for 30 min. 4T1 cells were then cocultured with macrophages, which were preincubated with serum-free DMEM in 7.5% CO_2 at 37 °C for 2 h. The mixed culture plates were then spun at 1000 rpm for 1 min and incubated at 37 °C for 2 h. After gently washing away any tumor cells that had not been phagocytized with PBS, the macrophages were fixed for 10 min with 1% formaldehyde and photographed using a Leica TCS 4D confocal microscope. The number of phagocytized cells stained

with CFSE per 100 macrophages was used to compute the phagocytic index [23].

Isolation of NK cells and NK cytotoxicity assays

The spleens of BALB/c mice were used to extract murine NK cells. After spleens were mechanically separated, Ficoll density gradient centrifugation was employed to separate mononuclear cells. Following a PBS wash, the Mouse NK Cell Isolation Kit II (130-096-892; Miltenyi Biotech, Auburn, CA, USA) was used to enhance the NK cells by negative selection. The cells were subsequently incubated with antibodies against NKp46-APC, CD3-FITC, and CD19-PE-Cy5 to verify the proper NK cell purification. The target cells were labeled for 90 min with 100 µCi of $^{51}Cr/10^6$ cells in 0.2 ml of culture medium in a 5% CO_2, 95% humidified atmosphere incubator at 37 °C. NK cells were added at the indicated target/effector ratios to determine the experimental release of ^{51}Cr (Perkin Elmer, Waltham, Massachusetts, USA). Then, the target cells were mixed with an equal volume of 2% Triton X-100 in PBS or an equal volume of media. to determine the maximum and spontaneous release of ^{51}Cr, respectively. The plates were then spun for 1 min at 1,000 rpm. NK cells and target cells were incubated for 4 h at 37 °C in 5% CO_2. Following incubation, the plates were centrifuged for 5 min at 2,000 rpm. A MicroBeta2 reader (Perkin Elmer) was used to measure the radioactivity after 100 µl of the supernatant was collected and combined with scintillation fluid. Specific killing (^{51}Cr release) was calculated using the following formula: 100 × (Experimental release - Spontaneous release)/(Maximum release - Spontaneous release) [9].

Isolation of $CD8^+$ cells and $CD8^+$ cytotoxicity assays

The functional activity of $CD8^+$ T cells was analyzed in order to ascertain whether vaccination with 4T1-luc2 cells could elicit an effective anti-breast cytotoxic T response. In summary, splenic $CD8^+$ T cells were isolated from mice that had been immunized with phosphate-buffered saline (PBS) (vehicle), non-irradiated 4T1-luc2 cells (5×10^5) or ex vivo irradiated 4T1-luc2 cells (5×10^5). Ten days after the stimulation, splenic $CD8^+$ T cells were isolated from immunized mice using a mouse $CD8a^+$ T cell Isolation Kit (Miltenyi Biotec). Non-irradiated 4T1-luc2 cells were used as specific target cells. The corresponding target cells (1×10^4/mL) were mixed at different ratios with effector cells overnight at 37 °C and detected using the Cytotoxicity Detection Kit LDH (Roche Applied Science, Basel, Switzerland) according to the manufacturer's protocol. Cytotoxicity of cytotoxic T lymphocytes was calculated according to the following formula: % cell lysis = (experimental– effector spontaneous– low control) x 100/(high control– low control); where, "experimental" corresponds to the experimental signal value, "effector spontaneous" to the spontaneous background signal value of the effector cells alone, "low control" to the spontaneous background signal value of target tumor cells alone, and "high control" to the maximum signal value of target cells in medium containing 1% Triton X-100. Cytotoxicity assays were performed for varying effector cell (E) to target cell (T) ratios, and specific cytotoxicity lysis percentages are reported as the mean ± SD of triplicate samples.

Depletion of $CD8^+$ T lymphocytes

For the $CD8^+$ T-cell depletion experiments, BALB/c mice were treated intraperitoneally with 250 µg of anti-CD8 (Bio-XCell, clone 2.43, BE0117) every 3 days. Following four treatments, peripheral blood was drawn and stained to use flow cytometry (FACSort cytometer, BD, Franklin Lakes, NJ, USA) to determine whether $CD8^+$ cytotoxic T lymphocytes were present among lymphoid cells.

Statistical analysis

Three measurements were made in triplicate for the experiments, and the mean ± S.D. was determined. Numerical data were analyzed to determine statistical significance via Mann–Whitney tests for comparisons of means via SPSS statistical software for Microsoft Windows, release 6.0 (Professional Statistic, Chicago, IL, USA). We used Student's two-tailed, unpaired t tests for individual comparisons. For every comparison, the significance level was set at $p < 0.05$. The Shapiro-Wilk test was used to check for normality.

Results

Ex vivo irradiation induces immune suppression of breast cancer lung colonization

To study the effect of IR on the immunogenicity of breast cancer cells, we designed a mouse model in which untreated or ex vivo-irradiated 4T1-luc2 cells were injected into the tail vein of immune competent BALB/c mice. Compared with the injection of untreated cells, the injection of irradiated cells resulted in a total reduction in the tumor load, not only in the lungs, the initial destination of the injected cells, but also at the point of cell injection. As shown in Figs. 1a and 100% of the animals injected with irradiated cells were free of disease, indicating an indefinite survival time.

To confirm that this effect was mediated by the immune system and was not due to a reduction in the viability and/or invasiveness of the irradiated cells, the same experiment was repeated on two immunodeficient mouse models (Fig. 1a and Fig. S1). We observed that injection of either non-irradiated or irradiated 4T1-luc2 cells was capable of inducing consistent tumors in the immunodeficient athymic nu/nu mouse model (Hsd: Athymic Nude-Foxn1nu), which lacks T cells but

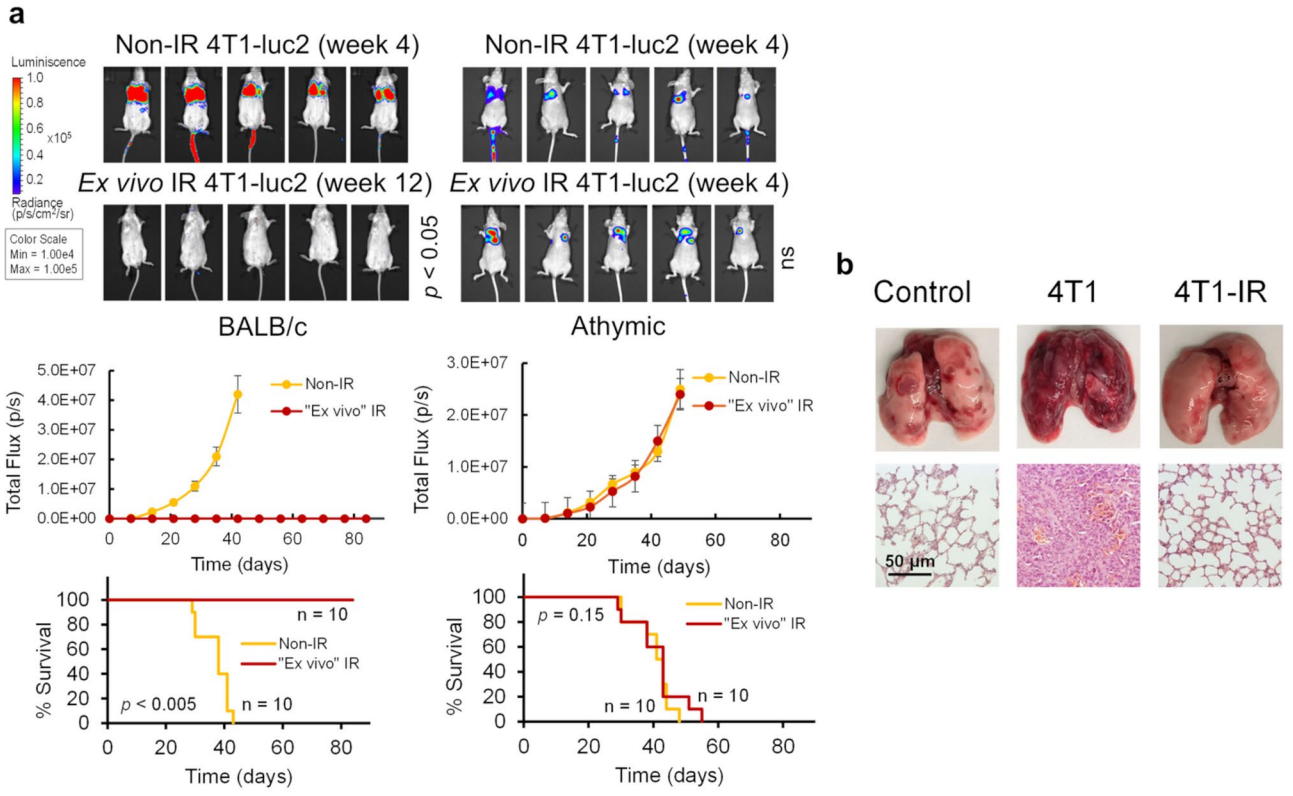

Fig. 1 The effect of ex vivo irradiation on the immune response against breast cancer cells. (**a**) Luciferase imaging of BALB/c and athymic mice injected with 4T1-luc2 cells via the tail vein. When indicated, the cells were irradiated ex vivo (10 Gy; 24 h). The total flux (photons/s) was compared between the ex vivo irradiated and non-irradiated groups (ns, not significant) and the histogram compares tumor evolution in groups injected with non-irradiated 4T1-luc2 (Non-IR) and ex vivo irradiated 4T1-luc2 ("Ex vivo"IR) cells. The values (mean ± S.D.) are representative of two independent experiments showing similar results ($n = 10$ for each experimental condition). Survival data are presented in the graph. (**b**) Lungs from BALB/c mice injected via the tail vein with vehicle (control) or the indicated cells (4T1-IR, ex vivo irradiated 4T1 cells). A microscopic view of the lung tissue structure (H&E stain, ×100) is shown below

maintains the functionality of B and NK cells, resulting in a significant decrease in survival time (Fig. 1a). In addition, 4T1-luc2 cells, when injected intravenously, were able to colonize the lungs of R2G2 mice, a double knockout mouse with an ultra-immunodeficient phenotype, independently of their irradiation status (Fig. S1).

As a control, and to rule out any potential immunogenicity due to the product of the luciferase gene, which is constitutively expressed in 4T1-luc2 cells, 4T1 parental cells were injected into the tail vein of immune competent BALB/c mice (Fig. 1b). The absence of tumors in the lungs of mice injected with irradiated 4T1 cells but not in the lungs of mice injected with untreated 4T1 cells, as demonstrated by H&E-stained histological samples, indicated that luciferase did not influence the immune response against the ex vivo irradiated breast cancer cells.

Ex vivo irradiation of breast cancer cells induces an adaptive immune response in mice and functions as a tumor vaccine

The decreased response in immunodeficient athymic nu/nu mice (Fig. 1a) was the first indication that irradiated cells elicit an anti-breast cancer immune response mediated in part by the adaptive immune response. Confirmation of this hypothesis was achieved via experiments in which 4T1-luc2 cells were injected via the tail vein of immune competent BALB/c mice depleted of $CD8^+$ T cells. We observed that efficient inactivation of $CD8^+$ T cells with a specific antibody (Fig. 2a) abolished the effect of irradiated cells in immunocompetent mice, resulting in tumor growth (Fig. 2b).

Immunological memory is an important characteristic of adaptive immunity. Since macrophage activation, following cancer cell-mediated phagocytosis, primes $CD8^+$ T cells to exhibit cytotoxic functions in vivo, we next developed a vaccination assay to test whether this response protects animals from tumor challenge. Thus, untreated 4T1-luc2 cells were injected into the breast pads of immunocompetent BALB/c mice that were immunized 4 weeks before tail vein injection of irradiated 4T1-luc2 cells. Our results showed that prior exposure to irradiated tumor cells substantially reduced the development of tumors from non-irradiated cells (Fig. 2c), suggesting a protective immune response against non-irradiated tumor cells.

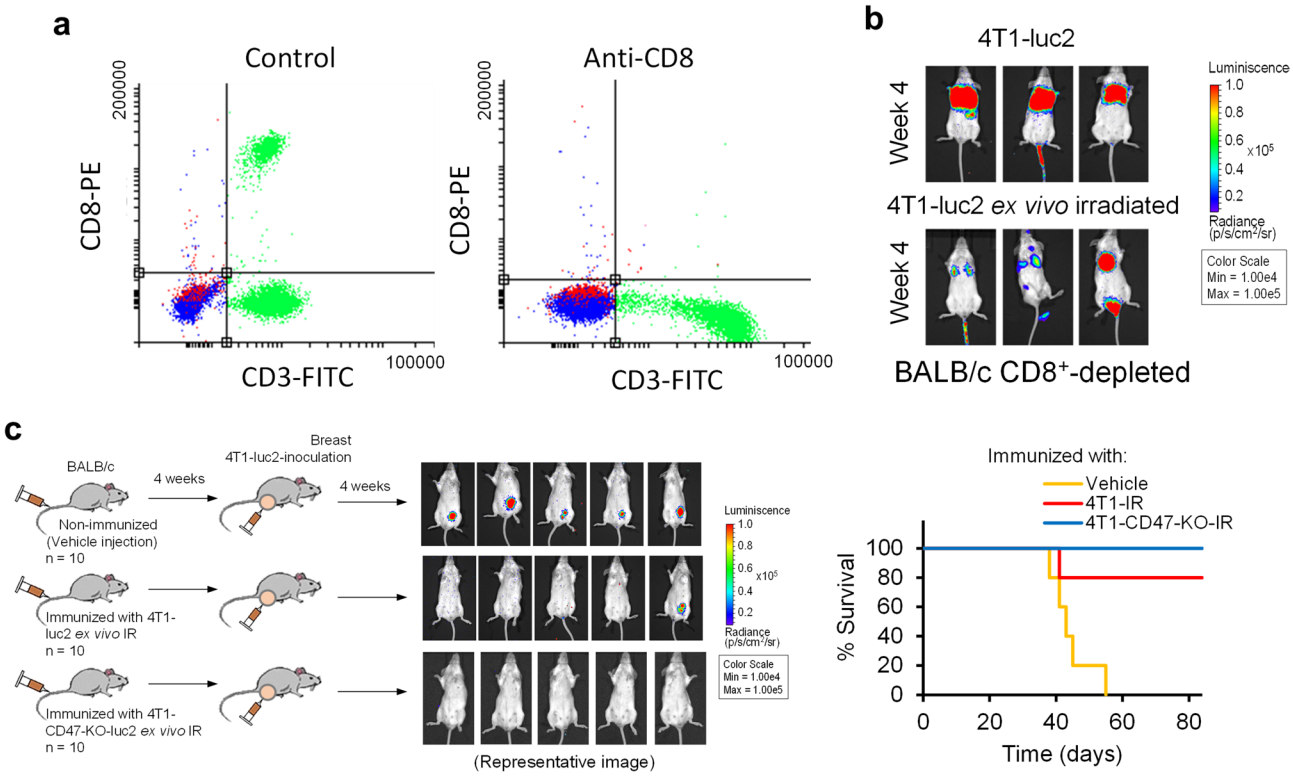

Fig. 2 Ex vivo irradiation of breast cancer cells induces an adaptive immune response. (**a**) Depletion of $CD8^+$ T lymphocytes. BALB/c mice were treated intraperitoneally with a dose (250 µg) of IgG isotype control (left panel) or anti-CD8-clone 2.43 (right panel) monoclonal antibody every 3 days. After four doses, peripheral blood was collected and stained to test for the presence of $CD8^+$ cytotoxic T lymphocytes among lymphoid cells by flow cytometry. The data show the complete clearance of T $CD8^+$ cells in a representative experiment out of two with similar results. The remaining blood cell counts (granulocyte, monocyte, NK and B lymphocyte counts) were unchanged (data not shown). (**b**) Inactivation of $CD8^+$ T cells in immunocompetent BALB/c mice results in tumor growth after the injection of 4T1-luc2 cells. The differences were significant ($p < 0.05$) compared with those of the BALB/c mice inoculated with ex vivo-irradiated 4T1-luc2 cells, as shown in Fig. 1A. (**c**) Vaccination assay. Non-immunized animals were injected with vehicle, while the immunized groups were injected with ex vivo-irradiated 4T1-luc2 cells (4T1-IR) or ex vivo-irradiated 4T1-CD47-KO-luc2 cells (4T1-CD47-KO-IR). After 4 weeks, non-irradiated 4T1-luc2 cells were injected intradermally. Analysis of primary tumors was carried out 4 weeks after breast pad injection. Differences between control and both immunized groups were statistically significant ($p < 0.05$). Survival was examined (right panel)

In order to ascertain the functional effect of ex vivo irradiated 4T1-luc2 cells on the ability to induce cytotoxic T lymphocytes, BALB/c mice were immunized with non-irradiated 4T1-luc2 cells, irradiated 4T1-luc2 cells or with PBS (vehicle). Following the harvesting of splenic $CD8^+$ T cells, a cytotoxicity assay was conducted. As shown in Fig. S2, the splenic $CD8^+$ T cells derived from the irradiated 4T1-luc2 cells immunized mice exhibited the strongest cytotoxic activity against target cells (14.6% killing; T:E ratio, 1:10) compared with $CD8^+$ T cells derived from both vehicle- and non-irradiated 4T1-luc2 cells-immunized groups (1% and 3.2%, respectively). The results demonstrate that $CD8^+$ T cells play a prominent role during memory immune responses in our experimental setting.

The site of injection of tumor cells as a determining factor for the activation of the immune system

The irradiation of cancer cells has been associated with a halt in their proliferation. Indeed, we observed that tumors formed by these irradiated 4T1 cells grew more slowly than those generated by non-irradiated cells (Fig. 3a). However, our previous results indicated that ex vivo 4T1-irradiated cells were able to induce breast cancer metastasis when injected into athymic mice (Fig. 1b). Similarly, we found that ex vivo 4T1-irradiated cells confined to the breast of immunocompetent mice also consistently formed breast tumors (Fig. 3a). Finally, these tumors spread to other organs, causing death (data not shown). We speculated that confinement of tumors in poorly irrigated tissues represents an impediment to efficient activation of the acquired immune system.

To test our hypothesis that ex vivo-irradiated 4T1 cells induce a potent immune response when injected into the bloodstream, we designed an intracardiac model in which tumor cells were directly injected into the arterial blood supply of BALB/c mice (Fig. 3b). Although cancer cells injected into the tail vein of mice are quickly directed to the lungs, in the intracardiac model, injected cells are first disseminated to multiple body organs

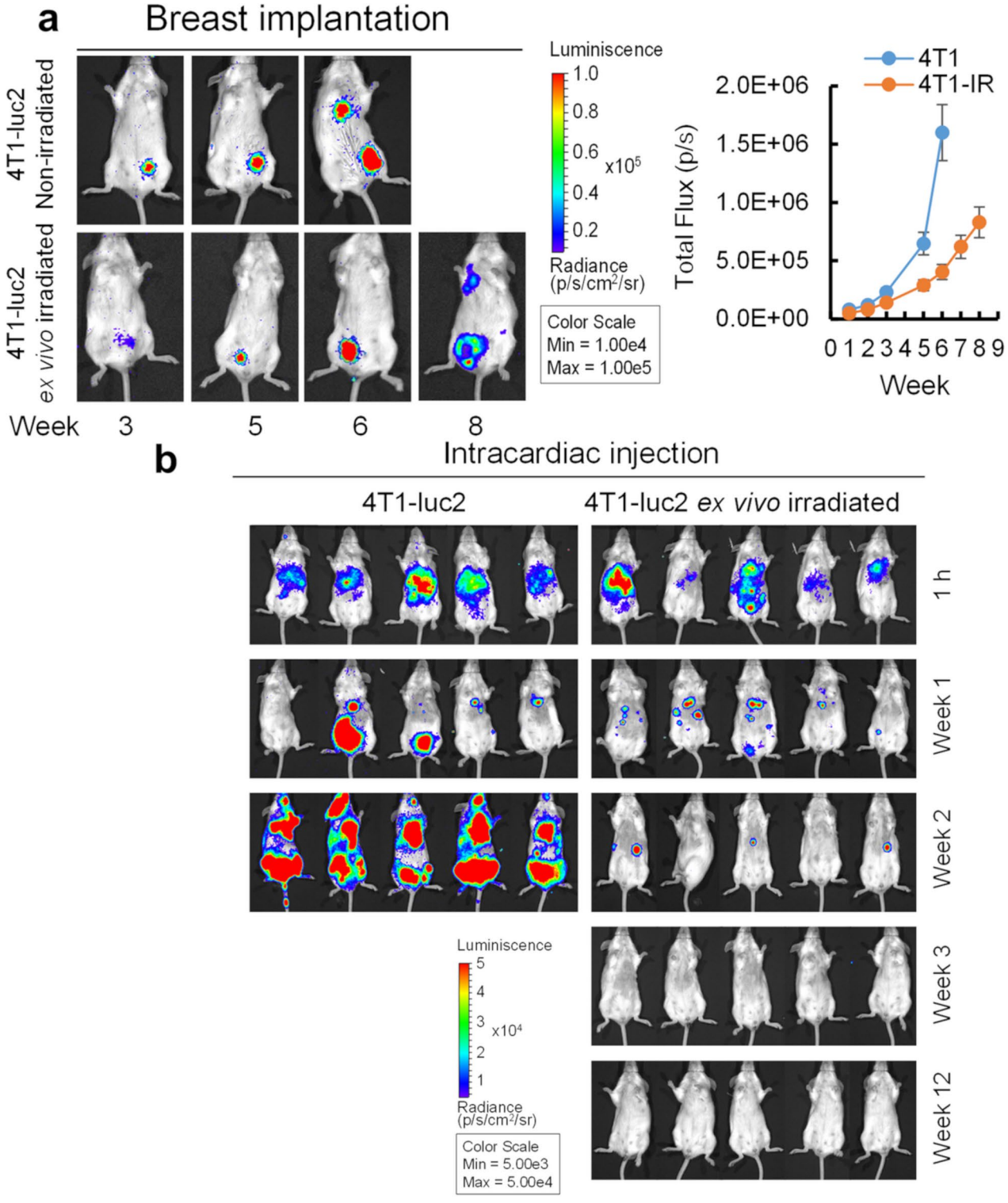

Fig. 3 The injection site of 4T1-luc2 cells determines the immune response in mice. (**a**) Luciferase imaging of a model where tumor cells were directly inoculated into the mammary path of BALB/c mice. 4T1-luc2 cells (both non-irradiated and ex vivo irradiated) induced primary tumor formation and metastasis in this mouse model. The histogram compares primary tumor evolution in groups injected with non-irradiated 4T1-luc2 (4T1) and ex vivo irradiated 4T1-luc2 (4T1-IR) cells. The values (mean ± S.D.) are representative of three independent experiments ($n = 10$ for each experimental condition). (**b**) Luciferase imaging of an intracardiac model where tumor cells were directly inoculated into the arterial blood supply of BALB/c mice. The images compare the evolution of tumors generated by injection of non-irradiated cells (4T1-luc2) versus those generated by injection of ex vivo irradiated cells (4T1-luc2 ex vivo irradiated)

before arriving at the lungs. In this case, we also observed a strong immune response after irradiated cell injection that was not observed in response to non-irradiated cells. Animals injected with non-irradiated 4T1-luc2 cells presented a multiorgan distribution of tumors, and they were sacrificed two weeks after cell injection due to obvious signs of disease. However, animals injected with ex vivo-irradiated 4T1-luc2 cells progressively recovered from the initially formed tumors. In fact, this last group did not show any obvious tumors three weeks after injection, and its follow-up for more than three months did not show any obvious signs of cancer-related disease (Fig. 3b). These data indicate that the easy accessibility of tumor cells is crucial for effective activation of the immune system and that ex vivo modification of tumor cells could increase their immunogenicity.

Engineering breast cancer cells to optimize macrophage-dependent phagocytosis

Next, we explored the capacity of IR to promote the phagocytosis of breast cancer cells by macrophages and performed in vitro phagocytosis assays. For this purpose, breast cancer cells were labeled with CFSE and cocultured with mouse PBMC-derived macrophages labeled with the red fluorescence dye PKH26 [23]. As shown in Fig. 4a, 4T1 cells were poorly agglutinated and phagocytized by macrophages; however, irradiated 4T1 cells were more efficiently phagocytized. As expected, blocking CD47 with a specific anti-CD47 antibody resulted in a significant increase in the phagocytosis of both irradiated and non-irradiated 4T1 cells by macrophages (Fig. 4a).

To improve the macrophage-dependent phagocytosis of 4T1 cells, we generated a CD47-knockout 4T1-luc 2 cell line using CRISPR-Cas9. The mutated sequence is shown in Fig. S3, and the lack of CD47 expression was detected by Western blot analysis. Interestingly, the knockout of CD47 in 4T1-luc2 cells did not have a strong effect on cell growth or viability, although it led to altered cell morphology (Fig. S3).

To examine the potential role of CD47 in the immune response to breast cancer, we compared the phagocytosis ratios of wild-type and 4T1-CD47-KO cells. The results revealed that depletion of CD47 in this murine cell line strongly increased the macrophage-dependent phagocytosis of non-irradiated 4T1 cells, although the maximal phagocytosis ratio was observed in irradiated 4T1-CD47-KO cells (Fig. 4b), probably due to IR-dependent exposure of the "eat me signal", CALR, at the plasma membrane (Fig. 4c). These results encouraged us to study the response of different animal models to tail vein injection of 4T1-CD47-KO cells.

Intravenous injection of CD47 knockout cells activates both the adaptive and innate immune systems

Activation of the adaptive immune system might consistently explain the longer lifespan of immunocompetent mice after intravenous injection of nonirradiated 4T1-CD47-KO cells than after injection of non-irradiated 4T1 cells (Fig. 1a *versus* Fig. 5a and b). However, the improved response of athymic mice to irradiated 4T1-CD47-KO cells (Fig. 1a versus Fig. 5a) may have a different explanation. In addition to inhibiting macrophage activation, CD47 transmits threshold-dependent direct inhibitory signals to activated NK cells via SIRPα [24]. Therefore, we investigated whether irradiated cells were able to activate NK cells in vivo. To this end, *ex vivo*-irradiated 4T1 or ex vivo-irradiated 4T1-CD47-KO cells were injected into the tail vein of athymic nude mice. After 1 week, NK cells from these mice were purified from their spleens and cocultured with YAC-1 cells or irradiated 4T1 cells. The results (Fig. 5c) revealed that intravenous injection of CD47 knockout cells significantly increased the activation of NK cells in athymic nude mice.

Ex vivo engineering of cells as an experimental therapy for breast cancer

As a proof of concept for the use of ex vivo manipulated breast cancer cells as a cellular therapy, we next analyzed whether vein tail injection of ex vivo irradiated 4T1-CD47-KO cells was able to eliminate 4T1-induced breast tumors. Untreated 4T1-luc2 cells were transplanted into the mammary glands of BALB/c mice to establish breast tumors, and after three weeks, the tumor-bearing mice were injected with ex vivo-irradiated 4T1-CD47-KO cells via the tail vein (Fig. 6a). The evolution of primary tumors was followed by in vivo luciferase imaging and compared with that of a vehicle-treated control group. In addition to a significant reduction in tumor growth, histological analyses also revealed that tumors derived from mice treated with ex vivo-irradiated 4T1-CD47-KO cells presented greater infiltration of $CD8^+$ T and NK cells than tumors obtained from vehicle-treated controls did (Fig. 6b). Importantly, tumors treated with irradiated 4T1-CD47-KO cells also presented a less immunosuppressive microenvironment, as evidenced by the significant reduction in the infiltration of Foxp3 + regulatory T cells (Tregs) (Fig. 6b).

Anti-PD1 therapy improves tumor recognition by activating immune cells

Although the growth of preformed mammary tumors in mice treated with ex vivo-irradiated 4T1-CD47-KO cells was significantly lower than that of tumors in untreated animals (Fig. 6a), these tumors eventually continued to grow and led to the death of all the mice (Fig. 6a). These

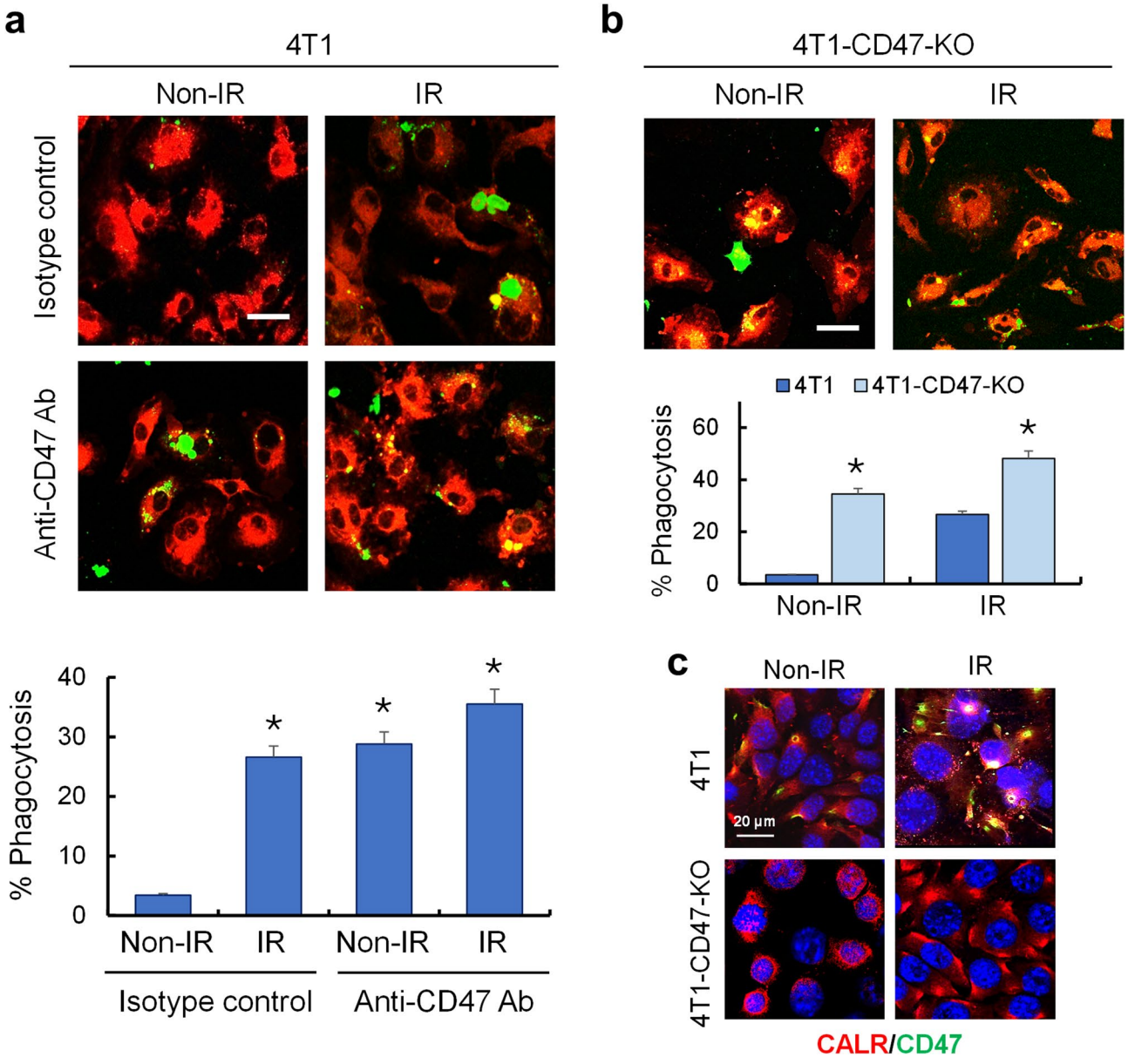

Fig. 4 Knocking down CD47 sensitizes breast cancer cells to macrophage phagocytosis. (**a**) CFSE-labeled 4T1-luc2 (4T1) irradiated (IR) or non-irradiated (non-IR) cells along with a blocking antibody against CD47 (B6H12.2, 10 µg/ml) were added to cultures of PKH26-labeled PBMC-derived macrophages. Two hours later, the cultures were washed and examined with an inverted confocal microscope. The data shown are representative microphotographs of three individual experiments. Green: CFSE-labeled melanoma cells; red: PKH26-labeled macrophages. Scale bar, 20 µm. The histogram shows the comparison of the phagocytosis index of macrophages against the indicated 4T1 cells. The phagocytosis index was calculated as the number of phagocytized $CFSE^+$ cells per 100 macrophages ($n = 3$, mean ± S.D.; $^*p < 0.05$ compared with the non-IR-isotope control group). (**b**) As in Fig. 4a, but CFSE-labeled 4T1-luc2-CD47-KO (4T1-CD47-KO) cells were used. The histogram shows the comparison of the phagocytosis index of macrophages against the indicated 4T1 cells ($n = 3$, mean ± S.D.; $^*p < 0.05$ compared with their respective 4T1 groups). Scale bar, 20 µm. (**c**) Confocal microscopy analysis of CD47 and CALR in 4T1 and 4T1-CD47-KO breast cancer cells under the indicated conditions

results contrast with those obtained in vaccination experiments with ex vivo irradiated 4T1-CD47-KO cells, where the implantation of tumor cells in immunized animals resulted in complete regression of these tumor cells in most of the animals, which resulted in an optimal percentage of survival (Fig. 2c).

Some background information, together with some observations made in our laboratory, seemed to indicate that the loss of complete effectiveness of these whole-cell treatments could be due to the expression of PD-L1 by tumor cells. PD-L1 expression is highly influenced by the tumor microenvironment [25]. Therefore, to determine the expression of PD-L1 in tumor-bearing mice,

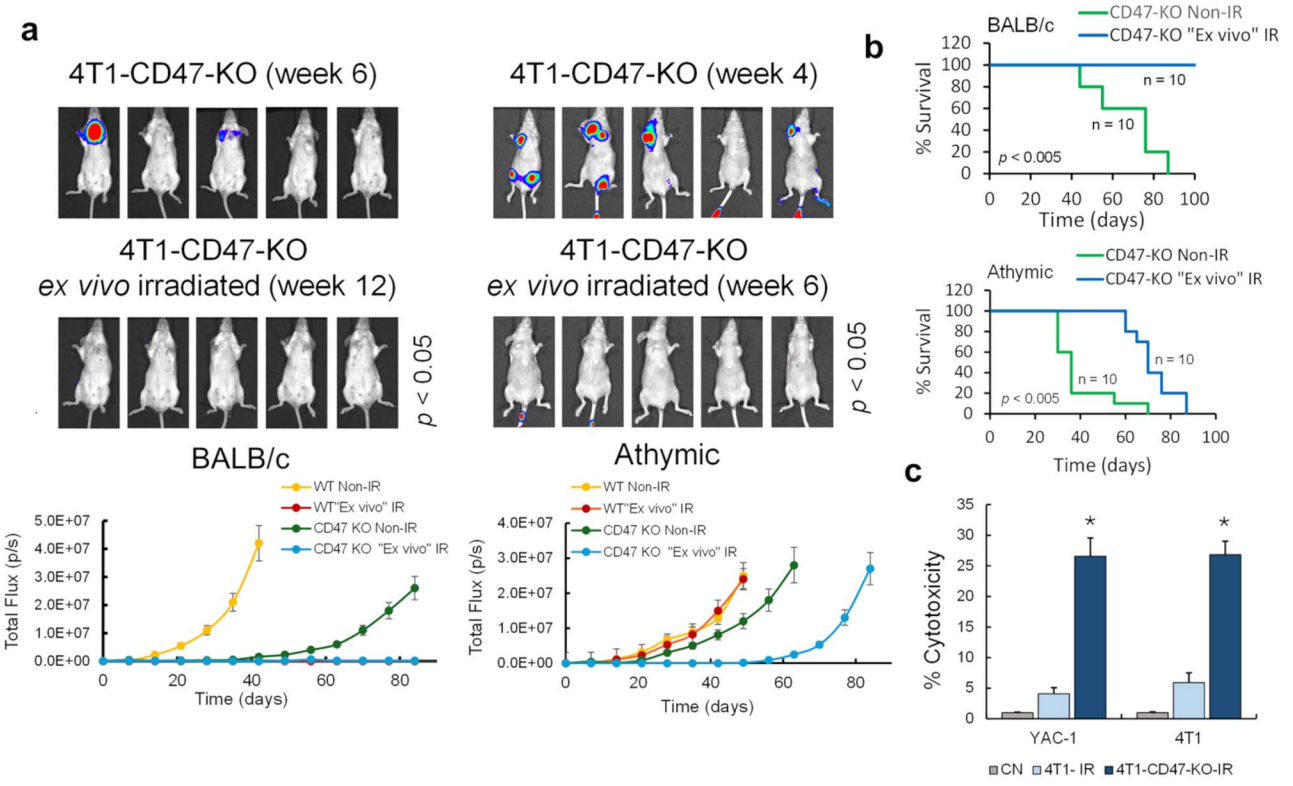

Fig. 5 Effect of CD47 depletion on the antibreast cancer immune response. (**a**) Luciferase imaging of athymic and BALB/c mice after tail vein injection of 4T1-CD47-KO cells. Where indicated, the cells were previously irradiated ex vivo (10 Gy; 24 h). The total flux (photons/s) was compared between the ex vivo irradiated and non-irradiated groups (*p* values). Color scale (Min = 1.00e6; Max = 1.00e7). Data of Fig. 1a, performed with irradiated or non-irradiated WT 4T1-luc2 cells expressing CD47, are used as a control for these experiments. The histogram compares tumor evolution in groups injected with non-irradiated 4T1-luc2 cells (both WT Non-IR and CD47-KO Non-IR) and ex vivo irradiated 4T1-luc2 cells (both WT "Ex vivo" IR and CD47-KO "Ex vivo" IR). The values (mean ± S.D.) are representative of two independent experiments showing similar results ($n = 10$ for each experimental condition). (**b**) Survival data for CD47-KO Non-IR and CD47-KO "Ex vivo" IR groups are presented (see Fig. 1a for comparative survival with WT control groups). (**c**) Athymic (Fox1nu) mice were immunized via tail vein injection with ex vivo-irradiated 4T1 and ex vivo-irradiated 4T1-CD47-KO breast cancer cells (10 Gy; 24 h). Control (CN) mice were injected with vehicle. One week after the injection, the animals were sacrificed, and NK cells were purified from their spleens. Purified NKs were cocultured with YAC-1 cells or irradiated 4T1 cells. NK cytotoxicity was evaluated by a ^{51}Cr release assay at an effector/target ratio (E/T) of 5. The results are representative of three independent experiments. *$p < 0.05$ compared with both the CN- and 4T1-immunized groups

we transplanted 4T1 cells into BALB/c mice (Fig. 7a). As shown in this figure, compared with 4T1 cells grown in in vitro cultures, 4T1-derived tumor cells presented increased expression of PD-L1 at both the mRNA and protein levels. This high microenvironment-dependent expression of PD-L1 could partly explain the efficient elimination of tumor cells in the vaccination experiments (Fig. 2c). Indeed, the activated immune system in immunized mice would have to eliminate 4T1 cells with reduced expression of PD-L1, whereas the preformed tumors used to test the efficacy of this cellular therapy exhibit high expression of PD-L1, which could inhibit their recognition by activated immune cells.

In addition, we also observed significant differences in PD-L1 expression between tumors from untreated control animals and those subjected to whole 4T1-CD47-KO-cell therapy (Fig. 7b). Although differences in the expression levels of PD-L1 in the tumors of treated and untreated animals could correspond to specific changes in the tumor microenvironment, the large reduction in the tumor volume of treated animals led us to hypothesize that the increased PD-L1 expression may be due to selective pressure derived from the therapy (Fig. 6a). Cells with high levels of PD-L1 are more resistant to destruction by immune cells, and their survival results in the clonal selection of PD-L1-positive cells.

To test this hypothesis, we performed therapies in which ex vivo-irradiated 4T1-CD47-KO cells were combined with an anti-PD-1 antibody to treat tumor-bearing mice (Fig. 7c). The complementary activity of each treatment was evident in the significant destruction of the tumor mass and extended survival of the animals treated with the combined therapy in comparison with those in the groups treated with the individual treatments.

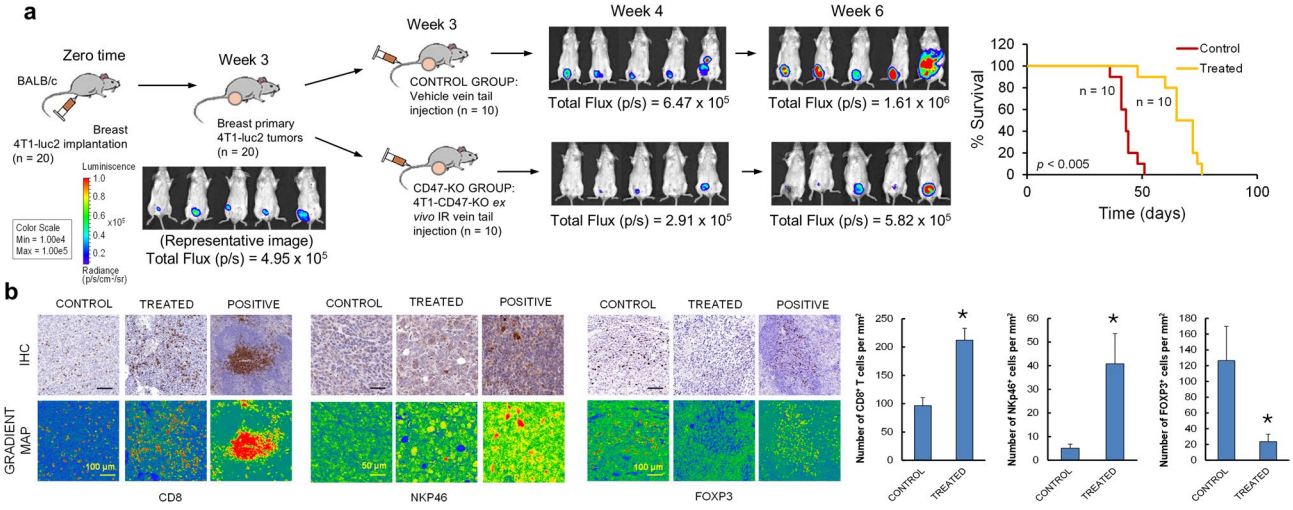

Fig. 6 Experimental cellular therapy for breast cancer. (**a**) 4T1-luc2 cells were transplanted into the mammary glands of BALB/c mice to establish breast tumors, and after three weeks, the tumor-bearing mice were divided into two groups. Animals in the control group were tail-injected with vehicle (PBS), while mice in the treated groups were injected with ex vivo-irradiated 4T1-CD47-KO cells (10 Gy; 24 h) via the tail vein. Luciferase imaging is shown. Color scale (Min = 1.00e6; Max = 1.00e7). The total flux (photons/**s**) was compared between the control and treated groups ($p < 0.05$ at both weeks 4 and 6). Survival data are presented in the graph. (**b**) IHC of 4T1 tumors obtained from the control and treated groups shown in Fig. 6a. Quantification was carried out by using ImageJ software (histograms) on three different areas of tumors and three animals per group (*$p = 0.005$). The gradient map highlights positive cells after immunostaining with CD8, NKp46, and FOXP3 antibodies. Positive controls for these immune cells were also included

Discussion

Several preclinical studies have demonstrated the synergistic effect of whole-cell-based vaccines combined with immune checkpoint inhibitors [26]. Most of these studies are based on immunization with whole cells derived from the immune system; however, the use of cellular vaccines derived from tumor cells is still rare. These studies have been delayed because of ethical issues in which the injection of tumor cells into humans could be ethically questionable. However, some of these ethical hurdles have been overcome in approving clinical trials using AGI-101 H, an allogeneic melanoma vaccine composed of two genetically modified human melanoma cell lines [8]. Perhaps ex vivo manipulation of these cells, i.e., irradiation with gamma rays to prevent the cells from proliferating, has been a critical issue to avoid the ethical barrier of this therapeutic treatment. Therefore, despite the logical ethical concerns that this therapy can generate for its use in humans, here, we advance in the design of an experimental whole tumor cell-based vaccine through its application in mouse models of breast cancer. We observed that the combination of this type of cell therapy with immune checkpoint inhibitors gave rise to more satisfactory results. Therefore, we worked with a two-stage strategy to increase the activation of the immune system while increasing the recognition of tumor cells by activating cytotoxic cells of the immune system.

The massive phagocytosis potential and antigen-presenting capabilities of macrophages make them crucial components of the innate immune system. However, the confinement of tumors in poorly vascularized areas, the tumor microenvironment and the presence of inhibitory signals on the surface of tumor cells are some of the impediments for macrophages to recognize and phagocytose tumor cells. Here, we observed that the injection of tumor cells into the bloodstream constitutes a rapid and direct way of enhancing the interaction between macrophages and tumor cells; however, despite enhancing the physical interaction between tumor cells and phagocytic cells, an optimal balance between "eat me" and "do not eat me" signals on the surface of tumor cells is an important determinant of phagocytic cellular uptake [11]. Thus, while the surface expression of CALR promotes the phagocytic uptake of dying, stressed, and cancer cells [27], its prophagocytic function is inhibited by CD47, which has been described as an antiphagocytic signal in several human cancers, including breast cancer [28]. Here, we show that ex vivo manipulation of the CALR/CD47 balance in cancer cells and their subsequent intravenous injection in mice favored macrophage-dependent phagocytosis and induced strong antitumor immunity.

Effective immunotherapy must consider not only the proper activation of different components of the immune system but also the ability of these activated elements to recognize tumor cells distributed in different organs of cancer patients. In recent years, many studies have elucidated how some tumors can escape surveillance and destruction by the immune system [29]. Thus, PD-L1 is a critical "don't find me" signal that represents an adaptive immune resistance mechanism exerted by tumor cells in response to endogenous immune antitumor activity. Therefore, ex vivo-modified tumor cell therapies, which

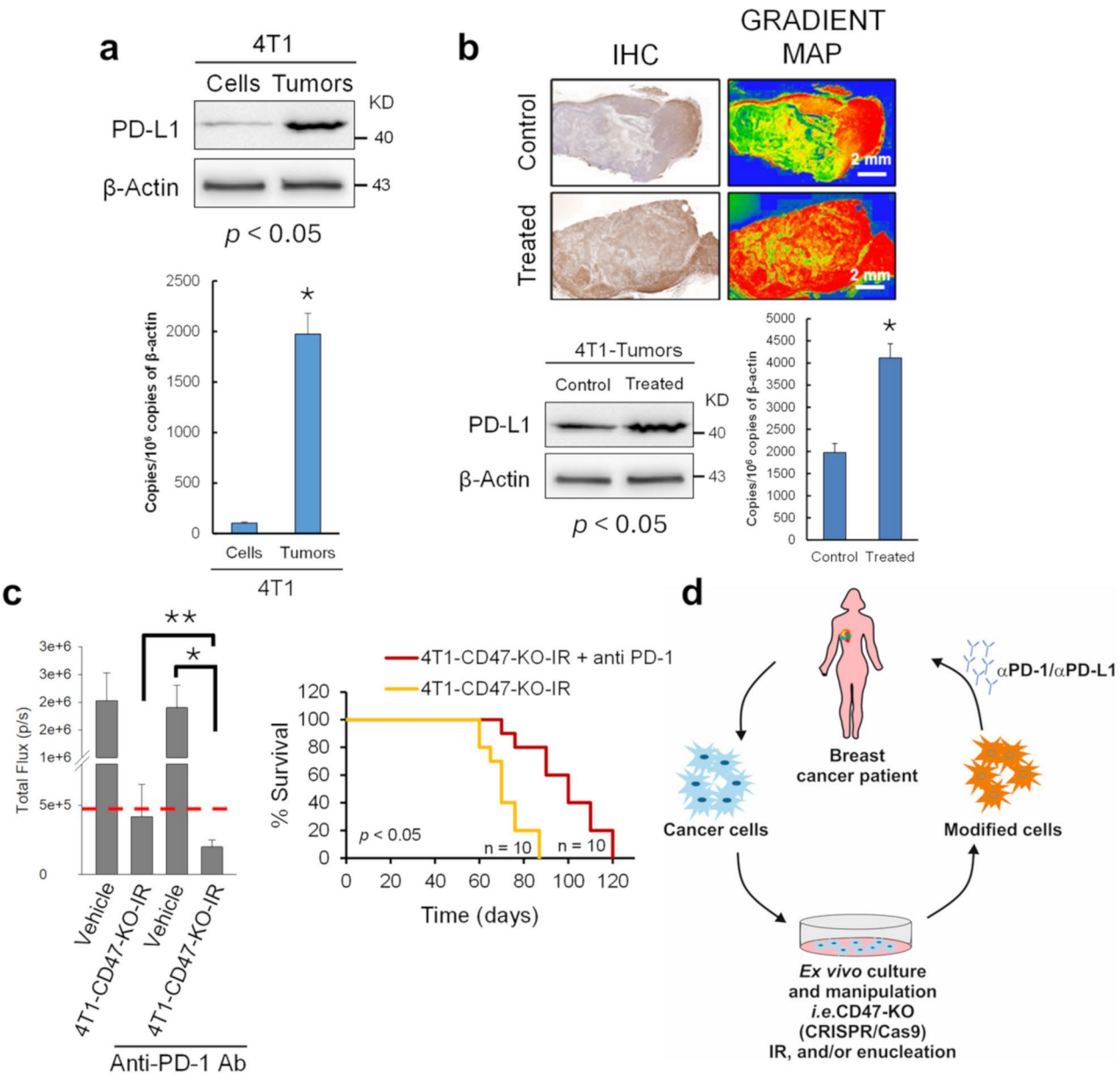

Fig. 7 The efficacy of combined anti-PD-1 therapy. (**a**) PD-L1 expression in 4T1 cells in culture (Cells) and in 4T1-induced tumors (Tumors) was analyzed by Western blotting and PCR (histogram), and the differences were statistically significant (*$p < 0.05$). For analysis of PD-L1 in solid tumors, we used those generated from the control group shown in Fig. 6a. The blots in this figure were cropped from different gels. The full blots are shown in Fig. S4. (**b**) Expression of PD-L1 in control and treated tumors generated in Fig. 6a. The expression of PD-L1 was analyzed by immunohistochemistry (IHC), Western blotting, and polymerase chain reaction (PCR) (histogram), and differences were found to be significant (*$p < 0.05$). The gradient map highlights positive cells after immunostaining with an anti-PD-L1 antibody. The full blots are shown in Fig. S4 (**c**). The model was established as described in Fig. 6a, and luciferase imaging at week 6 of the indicated treatments was used to determine the total flux (mean ± S.D.). When indicated, anti-PD-1 antibody (40 µg/mouse) was administered intraperitoneally via 3 doses on days 22, 26, and 30. The dashed red line indicates the average total flux at week 3 (before starting treatment); *$p < 0.005$; **$p < 0.05$. (**d**) A schematic representation for the cellular therapy proposed in this study. Ex vivo manipulated tumor cells from cancer patients could be used as a whole tumor cell-based vaccine for stimulate the recognition of body cancer cells by the immune system. In a second step, anti-PD-1/PD-L1 antibodies could be used to enhance the killing of tumor cells

ensure optimal activation of the immune system, are good candidates for combination treatment with immune checkpoint inhibitors such as anti-PD1/PD-L1 or other agents in the adjuvant or metastatic setting.

The results obtained in this study with preclinical mouse models could guide the design of personalized therapies in humans (Fig. 7d) where ideally, tumor cells obtained from surgical samples of a breast cancer patient could be cultivated and manipulated in vitro to make

them more immunogenic. These manipulated cells subsequently be injected into the same patient in combination with anti-PD1/PD-L1 therapy to achieve a strong response of the immune system toward the remaining cancer cells. Ideally, this combined therapy would be used in an adjuvant regimen after surgery to avoid the risk of relapses due to the presence of undetectable disease or in metastatic setting (unresectable tumors). Furthermore, it is important to note that this approach would have limited application in immunocompromised patients.

Despite the conceptual simplicity of this therapy, there are several methodological and ethical aspects that must be addressed for its translation to a clinical setting. For example, inoculation of a lysate of irradiated hepatocellular cancer cells inhibited tumor growth in a mouse model: however, no data are shown on whether vaccination protects mice against tumor challenge [30]. Another option could be the use of enucleated cells, it has been described that Cargocytes™ derived from hTERT-immortalized mesenchymal stem cells and engineered to express therapeutic levels of IL-12 can potently activate an antitumor immune response in a preclinical mouse model of triple-negative breast cancer [31, 32]. It would be interesting to know if bioengineering tumor cells devoid of a nucleus can maintain their ability to activate the immune system when they are injected intravenously. If this were the case, tumor cell-based therapies with enucleated cells could make these safe for patient administration and more compatible with current ethical standards.

Conclusion

Currently, great efforts are being made to improve existing cancer immunotherapy strategies, as well as to establish new cancer vaccine platforms and methods for discovering target antigens. Here, we used ex vivo manipulated breast cancer cells modified to improve in vivo phagocytosis as a cell-based vaccine in preclinical mouse models. We observed that this vaccine is a very good candidate for combination treatment with immune checkpoint inhibitors such as anti-PD1/PD-L1.

Abbreviations

APCs	Antigen-presenting cells
ATCC	American Type Culture Collection
CALR	Calreticulin
Cas9	CRISPR-associated protein 9
CD47	Cluster of differentiation 47
CFSE	Carboxyfluorescein succinimidyl ester
CRISPR	Clustered regularly interspaced short palindromic repeats
DCs	Dendritic cells
EMEM	Eagle's minimum essential medium
FBS	Fetal bovine serum
gRNA	Guide RNA
HDR	Homology-directed repair
H&E	Hematoxylin and eosin
IHC	Immunohistochemistry
IL-12	Interleukin-10
IR	Irradiation
KO	Knock-out
Luc	Luciferase
NK	Natural killer
PAM	Protospacer adjacent motif
PBMC	Peripheral blood mononuclear cells
PBS	Phosphate-buffered saline
PD-1	Programmed death–1
PD-L1	Programmed cell death ligand 1
qPCR	Quantitative PCR
RT–qPCR	Real-time quantitative PCR
RPMI	Roswell Park Memorial Institute
SDS–PAGE	Sodium dodecyl sulfate–polyacrylamide gel electrophoresis
SIRPα	Signal regulatory protein alpha
WT	Wild type

Supplementary Information

The online version contains supplementary material available at https://doi.org/10.1186/s12885-025-14432-1.

Supplementary Material 1

Acknowledgements

We thank Dr. Detlef Schuppan (Institute of Translational Immunology and Research Center for Immunotherapy, University Medical Center Mainz, Mainz, Germany) for providing the YAC-1 cell line and Prof. Yagita (Department of Immunology, Juntendo University School of Medicine, Japan) for providing the anti-PD-1 antibody.

Author contributions

Conceived and designed the experiments: JNRL and JCH. Performed the experiments: RMD, LSdC, MFM, JNRL, JCH, APM, and THC. Analyzed the data: JNRL, LSdC, JCH, and THC. Contributed reagents/materials/analysis tools: JNRL, JCH, APM, and THC. Wrote the paper: JNRL and JCH. The authors read and approved the final manuscript.

Funding

This work was supported by grants from the Ministerio de Ciencia, Innovación y Universidades (MICIU) [Projects PID2023-149281OB-I00 & CPP2023-010510 (MICIU/AEI/10.13039/ 501100011033 & FEDER, UE), and Fundación Séneca–Agencia de Ciencia y Tecnología de la Región de Murcia [FSRM/https://doi.org/10.13039/100007801(22544/PI/24). Spain]. R.M.D. has a fellowship from Fundación Séneca. Región de Murcia (Spain) (21407/FPI/20).

Data availability

The datasets generated and/or analyzed during the current study are available in the DIGITUM repository [http://hdl.handle.net/10201/151680].

Declarations

Ethics approval and consent to participate

Animals were bred and maintained according to Spanish legislation on the 'Protection of Animals used for Experimental and other Scientific Purposes' and in accordance with the directives of the European Community. All animal procedures were approved by the Ethical Committee of the University of Murcia and the Direccion General de Ganaderia y Pesca, Comunidad Autonoma de Murcia (Project reference A13151101).

Consent for publication

Not applicable.

Competing interests

The authors declare no competing interests.

Received: 27 February 2025 / Accepted: 2 June 2025
Published online: 01 July 2025

References

1. Guedan S, Calderon H, Posey AD Jr, Maus MV. Engineering and design of chimeric antigen receptors. Mol Ther Methods Clin Dev. 2018;12:145–56.
2. Sun D, She X, Li S, Wang X, Yang X, Wan M. CAR-T cell therapy: a breakthrough in traditional cancer treatment strategies. Mol Med Rep. 2024;29(3):47.
3. Ribas A, Comin-Anduix B, Chmielowski B, Jalil J, de la Rocha P, McCannel TA, et al. Dendritic cell vaccination combined with CTLA4 blockade in patients with metastatic melanoma. Clin Cancer Res. 2009;15(19):6267–76.
4. Saxena M, Bhardwaj N. Re-emergence of dendritic cell vaccines for cancer treatment. Trends Cancer. 2018;4(2):119–37.
5. Saxena M, van der Burg SH, Melief CJM, Bhardwaj N. Therapeutic cancer vaccines. Nat Rev Cancer. 2021;21(6):360–78.
6. Lin MJ, Svensson-Arvelund J, Lubitz GS, Marabelle A, Melero I, Brown BD, et al. Cancer vaccines: the next immunotherapy frontier. Nat Cancer. 2022;3(8):911–26.
7. Pérez-Baños A, Gleisner MA, Flores I, Pereda C, Navarrete M, Araya JP, et al. Whole tumour cell-based vaccines: tuning the instruments to orchestrate an optimal antitumour immune response. Br J Cancer. 2023;129(4):572–85.
8. Mackiewicz J, Burzykowski T, Iżycki D, Mackiewicz A. Re-induction using whole cell melanoma vaccine genetically modified to melanoma stem cells-like beyond recurrence extends long term survival of high risk resected patients - updated results. J Immunother Cancer. 2018;6(1):134.
9. Sánchez-Del-Campo L, Martí-Díaz R, Montenegro MF, González-Guerrero R, Hernández-Caselles T, Martínez-Barba E, et al. MITF induces escape from innate immunity in melanoma. J Exp Clin Cancer Res. 2021;40(1):117.
10. Stewart TJ, Abrams SI. How tumours escape mass destruction. Oncogene. 2008;27(45):5894–903.
11. Unanue ER. Perspectives on anti-CD47 antibody treatment for experimental cancer. Proc Natl Acad Sci USA. 2013;110(27):10886–7.
12. Park SY, Kim IS. Engulfment signals and the phagocytic machinery for apoptotic cell clearance. Exp Mol Med. 2017;49(5):e331.
13. Zhu M, Yang M, Zhang J, Yin Y, Fan X, Zhang Y, et al. Immunogenic cell death induction by ionizing radiation. Front Immunol. 2021;12:705361.
14. Tseng D, Volkmer JP, Willingham SB, Contreras-Trujillo H, Fathman JW, Fernhoff NB, et al. Anti-CD47 antibody-mediated phagocytosis of cancer by macrophages primes an effective antitumor T-cell response. Proc Natl Acad Sci USA. 2013;110(27):11103–8.
15. Casey SC, Tong L, Li Y, Do R, Walz S, Fitzgerald KN, et al. MYC regulates the antitumor immune response through CD47 and PD-L1. Science. 2016;352(6282):227–31.
16. Lian S, Xie R, Ye Y, Xie X, Li S, Lu Y, et al. Simultaneous blocking of CD47 and PD-L1 increases innate and adaptive cancer immune responses and cytokine release. EBioMedicine. 2019;42:281–95.
17. Park JJ, Thi EP, Carpio VH, Bi Y, Cole AG, Dorsey BD, et al. Checkpoint inhibition through small molecule-induced internalization of programmed death-ligand 1. Nat Commun. 2021;12(1):1222.
18. Han Y, Liu D, Li L. PD-1/PD-L1 pathway: current researches in cancer. Am J Cancer Res. 2020;10(3):727–42.
19. Patsoukis N, Wang Q, Strauss L, Boussiotis VA. Revisiting the PD-1 pathway. Sci Adv. 2020;6(38):2712.
20. Reck M, Rodríguez-Abreu D, Robinson AG, Hui R, Csőszi T, Fülöp A, et al. Pembrolizumab versus chemotherapy for PD-L1-positive non-small-cell lung cancer. N Engl J Med. 2016;375(19):1823–33.
21. Foerster F, Boegel S, Heck R, Pickert G, Rüssel N, Rosigkeit S, et al. Enhanced protection of C57 BL/6 vs balb/c mice to melanoma liver metastasis is mediated by NK cells. Oncoimmunology. 2017;7:e1409929.
22. Saenz L, Lozano JJ, Valdor R, Baroja-Mazo A, Ramirez P, Parrilla P, et al. Transcriptional regulation by poly(ADP-ribose) polymerase-1 during T cell activation. BMC Genomics. 2008;9:171.
23. Liu F, Jiang CC, Yan XG, Tseng HY, Wang CY, Zhang YY, et al. BRAF/MEK inhibitors promote CD47 expression that is reversible by ERK inhibition in melanoma. Oncotarget. 2017;8(41):69477–92.
24. Deuse T, Hu X, Agbor-Enoh S, Jang MK, Alawi M, Saygi C, et al. The SIRPα-CD47 immune checkpoint in NK cells. J Exp Med. 2021;218(3):e20200839.
25. Zheng NN, Zhou M, Sun F, Huai MX, Zhang Y, Qu CY, et al. Combining protein arginine methyltransferase inhibitor and anti-programmed death-ligand-1 inhibits pancreatic cancer progression. World J Gastroenterol. 2020;26(26):3737–49.
26. Oladejo M, Paulishak W, Wood L. Synergistic potential of immune checkpoint inhibitors and therapeutic cancer vaccines. Semin Cancer Biol. 2023;88:81–95.
27. Cockram TOJ, Dundee JM, Popescu AS, Brown GC. The phagocytic code regulating phagocytosis of mammalian cells. Front Immunol. 2021;12:629979.
28. Zhang H, Lu H, Xiang L, Bullen JW, Zhang C, Samanta D, et al. HIF-1 regulates CD47 expression in breast cancer cells to promote evasion of phagocytosis and maintenance of cancer stem cells. Proc Natl Acad Sci USA. 2015;112(45):E6215–23.
29. Gonzalez H, Hagerling C, Werb Z. Roles of the immune system in cancer: from tumor initiation to metastatic progression. Genes Dev. 2018;32(19–20):1267–84.
30. Chen J, Ding Y, Huang F, Lan R, Wang Z, Huang W, et al. Irradiated whole-cell vaccine suppresses hepatocellular carcinoma growth in mice via Th9 cells. Oncol Lett. 2021;21(5):409.
31. Wang H, Alarcón CN, Liu B, Watson F, Searles S, Lee CK, et al. Genetically engineered and enucleated human mesenchymal stromal cells for the targeted delivery of therapeutics to diseased tissue. Nat Biomed Eng. 2022;6(7):882–97.
32. Klemke RL, Wang H, Liu B, Alarcon C, Felicia Watson. Cargocytes: a novel cell therapy platform to drive anti-tumor immunity [abstract]. In: Proceedings of the, American Association for Cancer Research Annual Meeting, Atlanta GA. Philadelphia (PA): AACR; Cancer Res. 2019;79(13 Suppl):Abstract nr LB-067.

Publisher's note